

UCLA

UCLA Previously Published Works

Title

The Santa Ana Wildfire Threat Index: Methodology and Operational Implementation

Permalink

<https://escholarship.org/uc/item/4s84k92w>

Journal

Weather and Forecasting, 31(6)

ISSN

0882-8156

Authors

Rolinski, Tom
Capps, Scott B
Fovell, Robert G
[et al.](#)

Publication Date

2016-12-01

DOI

10.1175/waf-d-15-0141.1

Peer reviewed

The Santa Ana Wildfire Threat Index: Methodology and Operational Implementation

TOM ROLINSKI

U.S. Department of Agriculture Forest Service, Riverside, California

SCOTT B. CAPPS, ROBERT G. FOVELL, AND YANG CAO

University of California, Los Angeles, Los Angeles, California

BRIAN J. D'AGOSTINO AND STEVE VANDERBURG

San Diego Gas and Electric, San Diego, California

(Manuscript received 19 October 2015, in final form 30 June 2016)


ABSTRACT

Santa Ana winds, common to Southern California from the fall through early spring, are a type of down-slope windstorm originating from a direction generally ranging from $360^{\circ}/0^{\circ}$ to 100° and are usually accompanied by very low humidity. Since fuel conditions tend to be driest from late September through the middle of November, Santa Ana winds occurring during this time have the greatest potential to produce large, devastating fires upon ignition. Such catastrophic fires occurred in 1993, 2003, 2007, and 2008. Because of the destructive nature of such fires, there has been a growing desire to categorize Santa Ana wind events in much the same way that tropical cyclones have been categorized. The Santa Ana wildfire threat index (SAWTI) is a tool for categorizing Santa Ana wind events with respect to anticipated fire potential. The latest version of the index has been a result of a three-and-a-half-year collaboration effort between the USDA Forest Service, the San Diego Gas and Electric utility (SDG&E), and the University of California, Los Angeles (UCLA). The SAWTI uses several meteorological and fuel moisture variables at 3-km resolution as input to the Weather Research and Forecasting (WRF) Model to generate the index out to 6 days. In addition to the index, a 30-yr climatology of weather, fuels, and the SAWTI has been developed to help put current and future events into perspective. This paper outlines the methodology for developing the SAWTI, including a discussion on the various datasets employed and its operational implementation.

1. Introduction

From the fall through early spring, offshore winds, or what are commonly referred to as Santa Ana winds, occur over Southern California from the coastal mountains westward and from Ventura County southward to the Mexican border. These synoptically driven wind events vary in frequency, intensity, and spatial coverage from month to month and from year to year, thus making them difficult to categorize. Most of these wind events are associated with mild to warm ambient

surface temperatures $\geq 18^{\circ}\text{C}$ and low surface relative humidity $\leq 20\%$. However, during the late fall and winter months, these events tend to be associated with lower surface temperatures as a result of the air mass over the Great Basin originating from higher latitudes and other seasonal effects. There are a variety of ways to define a Santa Ana event through the analysis of local and synoptic-scale surface pressure and thermal distributions across Southern California (Raphael 2003). We view these offshore winds from a wildfire potential perspective, taking into consideration both the fuel characteristics and weather. As we have found, the index discussed herein provides a robust descriptor of both Santa Ana winds and the potential for wildfire activity. Used in conjunction with a mean sea level pressure (MSLP) map type, this is a powerful method for separating Santa Ana wind events from the more

 Denotes Open Access content.

Corresponding author address: Tom Rolinski, U.S. Forest Service, 2524 Mulberry St., Riverside, CA 92501.
E-mail: thomasrolinski@fs.fed.us

DOI: 10.1175/WAF-D-15-0141.1

© 2016 American Meteorological Society

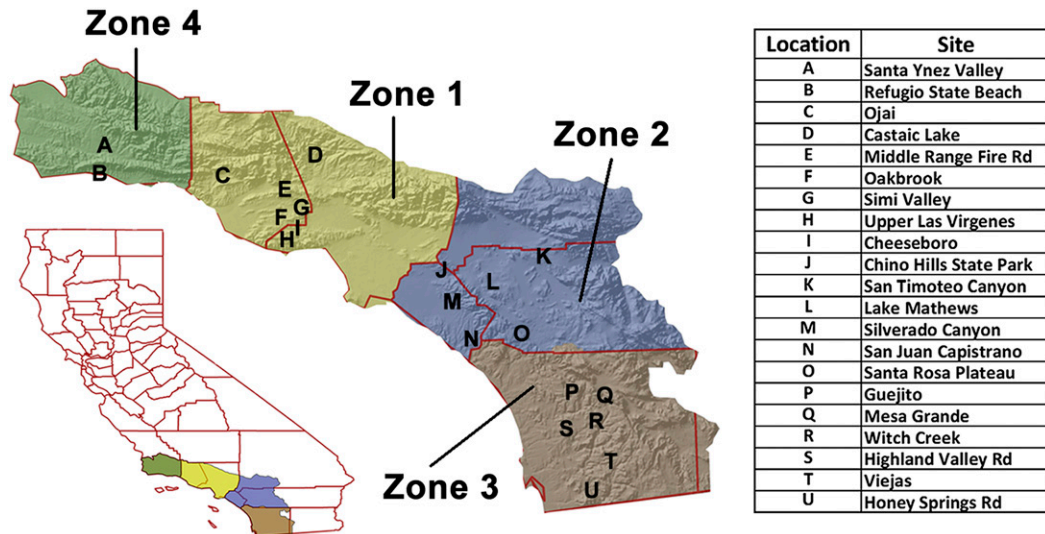


FIG. 1. Map of SAWTI zones. Inset shows SAWTI zones in reference to the state of CA. Letters denote locations of NDVI grassland sites with underlying topography shaded. Site names are provided in the lookup table to the right. County boundaries shown in red.

typical nocturnal offshore flows that occur throughout the coastal and valley areas (i.e., land breeze) during the year.

From 21 through 23 October 2007, Santa Ana winds generated multiple large catastrophic fires across Southern California (Moritz et al. 2010). Most notable was the Witch Creek fire in San Diego County, where wind gusts of 26 m s^{-1} were observed at the Julian weather station along with relative humidity values of $\approx 5\%$. However, high-resolution model simulations at 667 m showed that wind velocities were much higher in unsampled areas (Cao and Fovell 2016). This event became the catalyst for the development of a comprehensive Santa Ana wildfire potential index to better inform fire agencies, first responders, private industry, and the general public about the severity of an approaching event. This index could also help augment fire weather watches and red flag warnings from the National Weather Service by providing value-added information about an impending event.

The Predictive Services Unit, functioning out of the Geographic Area Coordination Center (GACC) in Riverside, California, is composed of several meteorologists employed by the USDA Forest Service. In 2009, Predictive Services began working on an index to categorize Santa Ana wind events according to the potential for a large fire to occur (Rolinski et al. 2011). This unique approach addresses the main impact Santa Ana winds can have on the population of Southern California beyond the causal effects of windy, dry weather. Following on, and improving upon this work, the Forest Service (through Predictive Services) collaborated

during a three-and-a-half-year period with the San Diego Gas and Electric utility (SDG&E) and the University of California, Los Angeles (UCLA), to develop the Santa Ana wildfire threat index (SAWTI). This index employs a gridded 3-km model to not only assess meteorological conditions, but also incorporates an estimation of fuel moisture to determine the likelihood of rapid fire growth during Santa Ana winds.

The SAWTI domain covers the coastal, valley, and mountain areas of Southern California from Point Conception southward to the Mexican border. This area has been divided into four zones based in part on the different offshore flow characteristics that occur across the region (Fig. 1). Zone 4, which covers Santa Barbara County and was the last zone to be included into the index (thus the reason for the discontinuity within the sequential order of zones going from north to south), does not typically experience Santa Ana winds in the classic sense. Strong northwest-to-north winds in this zone can either precede a Santa Ana wind event or can occur independently (typically in the summer), which in the latter case are more commonly known as “sundowners” (Blier 1998). In both cases, these downsloping winds are common to the south slopes of the Santa Ynez Mountains, an east–west coastal range that runs parallel to, and a few miles inland from, the shoreline. Although not frequent, significant fire activity associated with these winds in this zone has occurred in the past, which is why this geographic area is now represented in the index. Santa Ana winds across zones 1 and 2 are primarily a result of offshore surface pressure gradients (locally and/or synoptically) interacting with the local

terrain to produce gap winds through the Soledad Canyon, the Cajon Pass, and the Banning Pass (Hughes and Hall 2010; Cao and Fovell 2016). These winds also tend to precede the Santa Ana winds that occur across San Diego County by 12–24 h. Across zone 3, offshore winds take on a more “downslope windstorm” characteristic driven largely by the tropospheric stability (Cao and Fovell 2016). Other factors that led to the division of the zones were changes in terrain, National Weather Service Forecast Office boundaries, and local news media market areas. The SAWTI is more than a tool for meteorologists and fire agency managers to assess the severity of Santa Ana winds; it is also a tool for the general public to help better prepare for impending events that could lead to catastrophic fires. Therefore, the idea of displaying the product via zones keeps the index simple and easy to understand for all user groups. The following discussion centers around the assessment of fire potential related to Santa Ana winds, the methodology behind the weather and fuel components of the index, and its operational implementation.

2. Methodology

a. Large fire potential: Weather component

We define a large fire within the four SAWTI zones to be 100 ha. The potential for an ignition to reach or exceed this value depends on a number of components, for example, various meteorological and fuel conditions, suppression strategy, topography, accessibility, and resource availability. We achieved this threshold by employing a historical fire database that was constructed by Predictive Services. This database was assembled by collecting fire occurrence data (1990–2013) from all state and federal fire agencies within the confines of California. For example, some of the fire agencies include the USDA Forest Service, the Bureau of Land Management, the National Park Service, and the California Department of Forestry and Fire Protection (CALFIRE) to mention a few. This database contains information such as ignition date, acres burned, containment date, etc., and contains 32 683 records. The value of 100 ha was achieved by determining what the largest fire was for each day within the database and then taking the 95th percentile of all daily largest fires. The determination of this semiempirical threshold was also guided by decades of experience guiding coordinated attacks on wildfires throughout Southern California. Moreover, in most cases when this threshold is exceeded, the GACC becomes engaged in resource mobilization to assist in fire suppression. Current methods for evaluating fire potential include various indices from

the National Fire Danger Rating System (NFDRS; Bradshaw et al. 1983) and from the Canadian Forest Fire Danger Rating System (CFFDRS; Preisler et al. 2008). The Fosberg fire weather index (FFWI) is one such metric and is a function of wind speed, humidity, and temperature with output values ranging from 0 to 100 (Fosberg 1978). While the FFWI may show elevated output values for a Santa Ana wind event, it can also show elevated values for any day therefore making it too generic for our purposes.

Assuming an aggressive suppression strategy is employed with adequate resource availability in an easily accessible area, large fire potential (LFP) can be simplified into a function involving fuel and meteorological conditions preceding, during, and following the time of ignition. From observation and experience, the two weather variables that contribute most toward fire growth during a Santa Ana wind event are wind velocity and the amount of dry air present near the surface. To illustrate this concept, we examined the difference between two Southern California fire regimes (Jin et al. 2015) consisting of fire activity during the summer, versus only during the fall when Santa Ana winds begin to increase in frequency (Figs. 2 and 3). It is easy to see that most of the fire activity during the summer occurs in low-wind situations with varying dewpoint depression values. However, fires burning in the autumn are commonly associated with stronger winds and higher dewpoint depression values. Therefore, based on operational experience, observations, and model data, we believe the potential for a new ignition to reach or exceed 100 ha based solely on weather conditions during a Santa Ana wind event is best expressed by the following equation:

$$\text{LFP}_w = 0.001W_s^2D_d, \quad (1)$$

where W_s is the near-surface (10 m AGL) sustained wind speed (m h^{-1}) and D_d is the near-surface dewpoint depression ($^{\circ}\text{F}$). It should be noted that this equation was validated by examining dynamically downscaled reanalysis data across Southern California for the month of October from 1979 to 2010. It has been suggested that wind speed has an exponential effect on the spread of fire among finer fuels such as grass and brush, and that wind can also have the same effect on fire spread as a fire burning upslope with little or no wind (Rothermel 1972). Dewpoint depression ($T - T_d$) depicts the dryness at the surface well and affects the moisture content of vegetation. Also, dewpoint depression can sometimes differentiate better between warm and cold offshore events than relative humidity can. In our dataset, it has been noted that larger dewpoint depression values ($D_d \geq 24^{\circ}\text{C}$) have

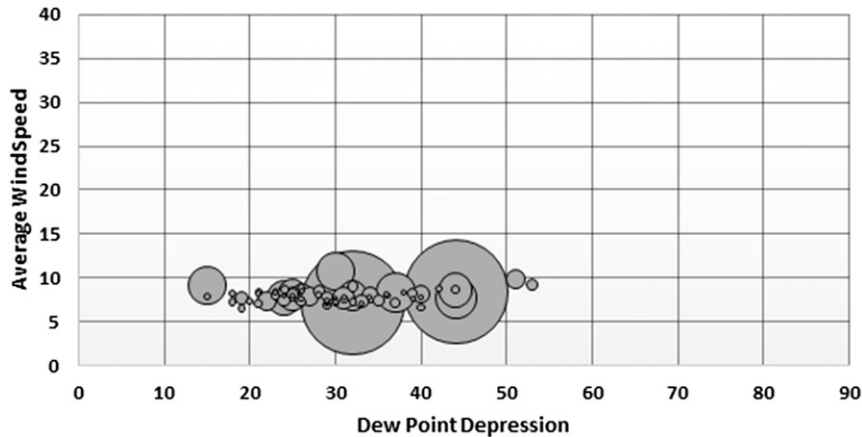


FIG. 2. Relationship of large fire (≥ 100 ha) occurrence and relative size with respect to average wind speed and dewpoint depression across zone 1 between 1 Jun and 20 Sep from 1992 to 2012. Bubble size represents relative fire size.

mainly been associated with warm events. While this may seem trivial, cold Santa Ana wind events (surface ambient temperatures $< 16^{\circ}\text{C}$) are usually not associated with large fires (according to our historical fire database previously mentioned). This may be due in part to lower fuel temperatures because in those cases more time would be needed to reach the ignition temperature. Another reason is that colder events are sometimes preceded by precipitation either by a few days or by a few weeks, which would cause fuels to be less receptive to new ignitions. These are the primary reasons why temperature was excluded from (1), although it has been incorporated indirectly through the use of D_d and in the fuels component that will be discussed in the following section. Finally, we note that while (1) bears some resemblance to the FFWI, a comparison of daily outputs of FFWI and LFP_w revealed that LFP_w provides significantly greater contrast between Santa Ana days and non-Santa Ana days. Therefore,

these results favored LFP_w as being the more appropriate equation for our purposes.

b. Large fire potential: Fuel moisture component

In addition to the meteorological conditions, LFP is also highly dependent on the state of the fuels. Given the complexity of the fuel environment (i.e., fuel type, continuity, loading, etc.), we decided to focus more specifically on fuel moisture since that aspect plays a critical role in the spread of wildfires (Chuvieco et al. 2004). For our purposes, we have condensed fuel moisture into three parameters: 1) dead fuel moisture, 2) live fuel moisture, and 3) the state of green-up of the annual grasses. Each of these aspects of fuel moisture is complex and will be defined more specifically later. We combined these moisture variables into one term, which we refer to as the fuel moisture component (FMC). While the variables within the FMC often act in concert with each other, there are times when they are out of

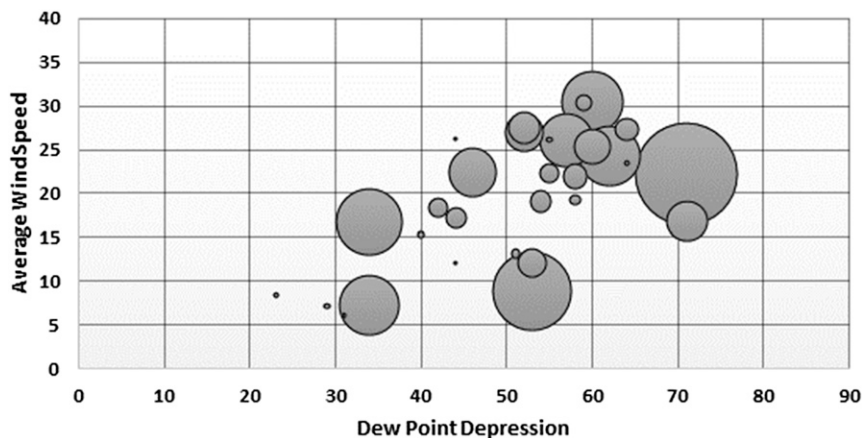


FIG. 3. As in Fig. 2, but between 21 Sep and 31 Dec.

phase with one another as a result of the variability in precipitation (frequency and amount) that occurs across Southern California during the winter. Through a comprehensive empirical investigation, the governing equation for FMC can be expressed as

$$\text{FMC} = \left\{ 0.1 \left[\left(\frac{\text{DL}}{\text{LFM}} - 1 \right) + G_{\text{ag}} \right] \right\}^{1.7}, \quad (2)$$

where DL is the dryness level consisting of the energy release component (ERC) and the 10-h dead fuel moisture time lag $\text{DFM}_{10\text{hr}}$. Dead fuel refers to nonliving plant material whose moisture content responds only to ambient moisture. Dead fuel is typically grouped into “time lag” classes according to diameter as follows: 0.20 cm, $\text{DFM}_{1\text{hr}}$; 0.64 cm, $\text{DFM}_{10\text{hr}}$; 2.00 cm, $\text{DFM}_{100\text{hr}}$; and 6.40 cm, $\text{DFM}_{1000\text{hr}}$. Live fuel moisture (LFM) is a sampling of the moisture content of the live fuels indigenous to the local region, and G_{ag} is the degree of green-up of the annual grasses. Currently, we are making the assumption that all the terms in (2) have equal weight, but further study may lead to future modifications.

1) DRYNESS LEVEL

The DL is a function of ERC and $\text{DFM}_{10\text{hr}}$ calibrated to historical fire occurrence across Southern California with unitless values ranging from 1 to 3. ERC is a relative index of the amount of heat released per unit area in the flaming zone of an initiating fire and is composed of live and dead fuel moisture as well as temperature, humidity, and precipitation (Bradshaw et al. 1983). While ERC is a measure of potential energy, it also serves to capture the intermediate- to long-term dryness of the fuels with unitless values generally ranging from 0 to 100 (using NFDRS fuel model G). The $\text{DFM}_{10\text{hr}}$ represents fuels in which the moisture content is exclusively controlled by environmental conditions (Bradshaw et al. 1983). Output values of $\text{DFM}_{10\text{hr}}$ are in grams per gram expressed as a percentage ranging from 0 to 60. In the case of the $\text{DFM}_{10\text{hr}}$, this is the time required for dead fuels (0.64–2.54 cm in diameter) to lose approximately two-thirds of their initial moisture content (Bradshaw et al. 1983). Thus, a DL of 1 indicates that dead fuels are moist, 2 represents average dead fuel dryness, and a 3 indicates that the dead fuels are drier than normal.

2) LIVE FUEL MOISTURE

The observed LFM is the moisture content of live fuels (e.g., grasses, shrubs, and trees) expressed as a ratio of the weight of water in the fuel sample to the oven dry weight of the fuel sample (Pollet and Brown 2007). Soil moisture as well as soil and air temperature govern the physiological activity, which results in changes in fuel

moisture (Pollet and Brown 2007). LFM is a difficult parameter to evaluate because of the irregularities associated with observed values. For instance, samples of different species of native shrubs are normally taken twice a month by various fire agencies across Southern California. However, the sample times often differ between agencies and the equipment used to dry and weigh the samples may vary from place to place. In addition, sample site locations are irregular in their distribution and observations from these sites may be taken sporadically. This presents a problem when we attempt to assess LFM over the region shown in Fig. 1.

Apart from taking fuel samples, there are several ways of estimating LFM using meteorological variables, soil water reserves, solar radiation, etc. (Castro et al. 2003). In particular, we developed an approach to modeling the LFM of chamise or greasewood (*Adenostoma fasciculatum*), a common shrub that grows within the chaparral biome in Southern California and is particularly flammable because of its fine, needlelike leaves and other characteristics (Countryman and Philpot 1970; Fovell et al. 2016, manuscript submitted to *Int. J. Wildland Fire*). This strategy makes use of historically observed LFM data from 10 sampling sites across Southern California and soil moisture from the 40–100-cm layer ($\text{SMOIS}_{40-100\text{cm}}$) from the North American Land Data Assimilation System, phase 2 (NLDAS-2). At each sampling site, LFM deviations from climatology are predicted using $\text{SMOIS}_{40-100\text{cm}}$ departures from its own annual cycle. A key element of the model is the incorporation of a 22-day lag between $\text{SMOIS}_{40-100\text{cm}}$ and LFM that improved the model fits. This is because a certain period of time elapses during which water percolates downward through the soil layers and then is drawn back up through the root system of the plant. This time can vary between 4 and 43 days depending on the evaporative conditions, soil structure, and site elevation. An average of this time lag over all the stations equated to 22 days. Current LFM values observed are relatable to gridded NLDAS-2 soil moisture anomalies from about 3 weeks earlier.

That approach, although quite skillful, results in site-specific equations not easily generalized across Southern California. The SAWTI index presently makes use of a simplified version of this strategy, applied to all grid points in the domain. For a given day, the model can be expressed as

$$\text{LFM} = (\text{SMOIS}_{40-100\text{cm}22\text{days}} - \text{SMOIS}_m) + 82, \quad (3)$$

where $\text{SMOIS}_{40-100\text{cm}22\text{days}}$ is the soil moisture of the 40–100-cm layer from 22 days earlier and SMOIS_m is the mean soil moisture from 2009 to 2012 for that same date.

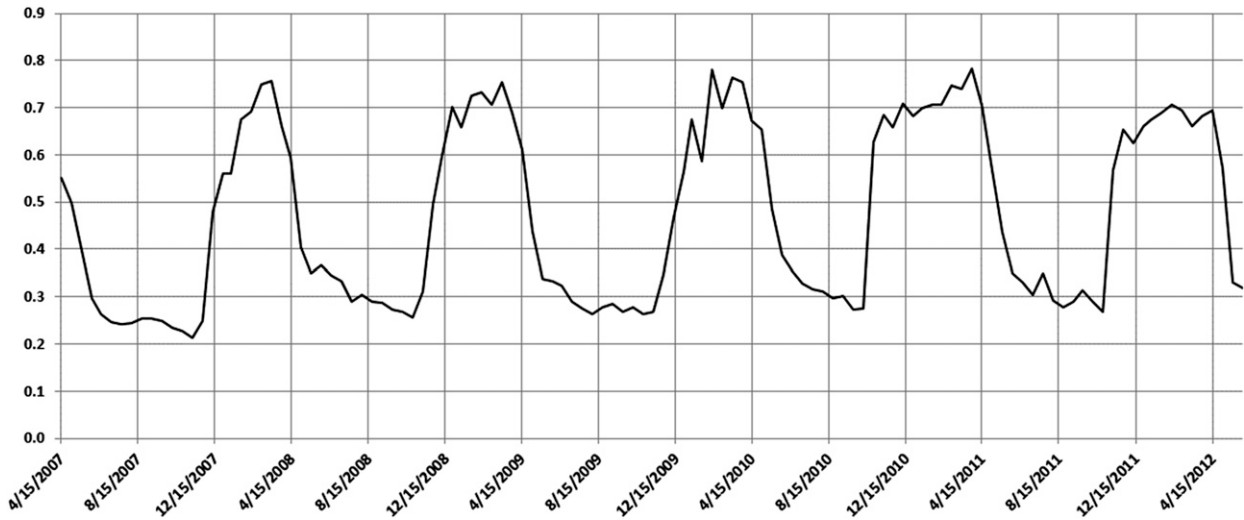


FIG. 4. Sample annual NDVI output.

The empirically selected constant of 82 roughly approximates the annual mean LFM over a large variety of sites.

3) ANNUAL GRASSES G_{ag}

Following the onset of significant wetting rains, new grasses will begin to emerge in a process called green-up. While the timing and duration of this process fluctuate from year to year, some degree of green-up usually occurs by December across Southern California. During the green-up phase, grasses will begin to act as a heat sink, thereby preventing new ignitions and/or significantly reducing the rate of spread among new fires. By late spring these grasses begin to cure with the curing phase normally completed by mid-June. In (2), G_{ag} is a value that quantifies the said green-up and curing cycles of annual grasses.

The value of G_{ag} is derived from the Moderate Resolution Imaging Spectroradiometer (MODIS) NDVI dataset at a resolution of 250 m for select pixels consisting solely of grasslands. NDVI is further defined by red and near-infrared (NIR) bands in the following equation:

$$NDVI = \frac{\rho_{NIR} - \rho_b}{\rho_{NIR} + \rho_b}, \quad (4)$$

where b is the reflectance in band b (Clinton et al. 2010). It can be shown that NDVI values for Southern California grasslands generally range from about 0.25 (± 0.05) to 0.75 (± 0.05) for an average rainfall year (Fig. 4). There is evidence that NDVI is affected by soil color (Elmore et al. 2000), which may explain the NDVI differences (± 0.05) seen among the selected Southern California grassland locations.

We give G_{ag} a rating of from 0 to 5 based on NDVI data, where 0 is green and 5 is fully cured. When

applying the methodology discussed by White et al. (1997) to the general range of Southern California grasslands, green-up is estimated to have occurred when NDVI exceeds 0.50. However, we have found that this value can be closer to 0.64 for some sites, and therefore NDVI values greater than 0.64 are assigned a value of 0, or green. Furthermore, NDVI values less than or equal to 0.39 are assigned a value of 5. This is because NDVI values are observed to be below 0.39 for all grassland sites during the dry season when grasses are known to be fully cured. A linear relationship exists between NDVI-derived values of G_{ag} and fire occurrence in Southern California (Fig. 5). For this reason, the transition between green and fully cured (or vice versa) was given a rating of from 1 to 4 in NDVI increments of 0.05 (Table 1).

To model NDVI, we used MODIS-derived NDVI biweekly data observed at 21 stations shown in Fig. 1, interpolated to daily frequency using cubic splines. The data availability period was January 2004–June 2012. For ease of implementation, our goal was to create a simple, yet skillful equation to capture the temporal variation of NDVI:

$$NDVI = \alpha + \beta_1 \cos(2\pi DOY/LOY) + \beta_2 PRECIP_{accum} + \beta_3 RH_{avg} + \beta_4 VEG_{frac} + \beta_5 SMOIS_{40-100cm}, \quad (5)$$

where DOY is the 1 January–based day of the year and LOY is the length of the year in days. The regressor $PRECIP_{accum}$ is the 1 September–based annually accumulated precipitation (mm), RH_{avg} is the 30-day running averaged relative humidity, VEG_{frac} is the surface vegetation fraction (0–1), and $SMOIS_{40-100cm}$ is the soil moisture content of the 40–100-cm depth ($kg\ m^{-3}$). This

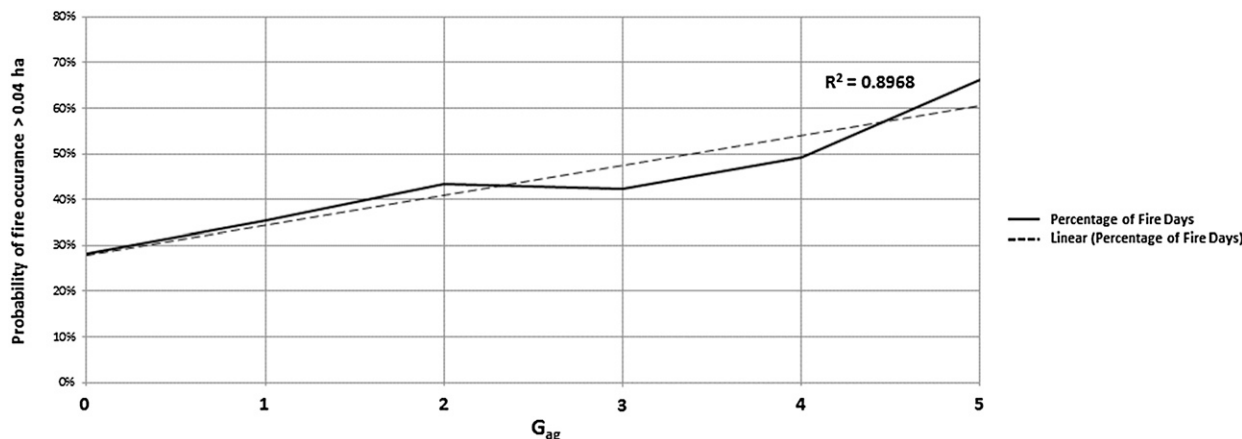


FIG. 5. Probability of fires ≥ 0.04 ha predicted by NDVI-derived G_{ag} for zone 3.

equation was the result of the “random forest” selection and stepwise regression applied to a large number of meteorological candidate regressors; see Cao (2015) for more information. The R^2 of the model is 0.73; see Table 2 for coefficient values.

We applied this model to the 21 sites in the four zones shown in Fig. 1. It is recognized that at some stations and times, the NDVI predictions are somewhat out of phase (i.e., the up and down ramps are too early or too late) with the observations, and the peaks are over- or underpredicted at different locations and times. The marked drought year of 2007 is clearly a problem at some locations, especially in zone 2. However, considering the fact that this is a simple universal model with only five regressors applied across Southern California, we believe it has shown adequate skill overall (Cao 2015).

c. Large fire potential: Weather and fuels

Given our derived expression for fuel characteristics, we can now predict large fire potential during Santa Ana wind events, taking into consideration both the weather and the fuels. FMC modifies (1) in cases where fuels have not fully cured and are still inhibiting fire spread. Output values of FMC range from 0 to 1, where 0 represents wet fuels and 1 denotes dry fuels. This modifier can become so influential that it will greatly reduce or

even eliminate the potential for large fire occurrence despite favorable meteorological conditions for rapid fire growth. So the final equation for large fire potential becomes

$$LFP = 0.001W_s^2D_dFMC. \tag{6}$$

The value of the incorporation of fuel moisture predictions into the index is illustrated in Fig. 6. For example, examination of the period between September 2008 and May 2009 shows a number of significant Santa Ana wind events indicated by the spikes in LFP_w . The difference between LFP_w and LFP is small during the fall months attributed to high FMC values. This is confirmed by viewing the relatively close spatial agreement between LFP_w and LFP (Fig. 7). In contrast, large differences occur after significant winter rains commence (Fig. 8). Large wildfires had occurred during each of the spikes noted in the fall while little fire activity was recorded despite the LFP_w spikes during January. This is precisely because of low FMC values, which illustrates the critical role that fuels play in this index.

3. Operational SAWTI

a. Model configuration

The data ingested to compute the four-zone, 6-day LFP operational forecasts come from multiple sources

TABLE 1. Relationship between NDVI and greenness.

NDVI	G_{ag} No.	Description
$NDVI > 0.64$	0	Green
$0.59 < NDVI \leq 0.64$	1	
$0.54 < NDVI \leq 0.59$	2	
$0.49 < NDVI \leq 0.54$	3	
$0.39 < NDVI \leq 0.49$	4	
$0 \leq NDVI \leq 0.39$	5	Cured

TABLE 2. Selected NDVI regressors.

Coef	Value
α	-0.314 867
β_1	0.112 535 92
β_2	1.44×10^{-5}
β_3	0.003 556 47
β_4	0.911 360 168
β_5	0.002 412 815

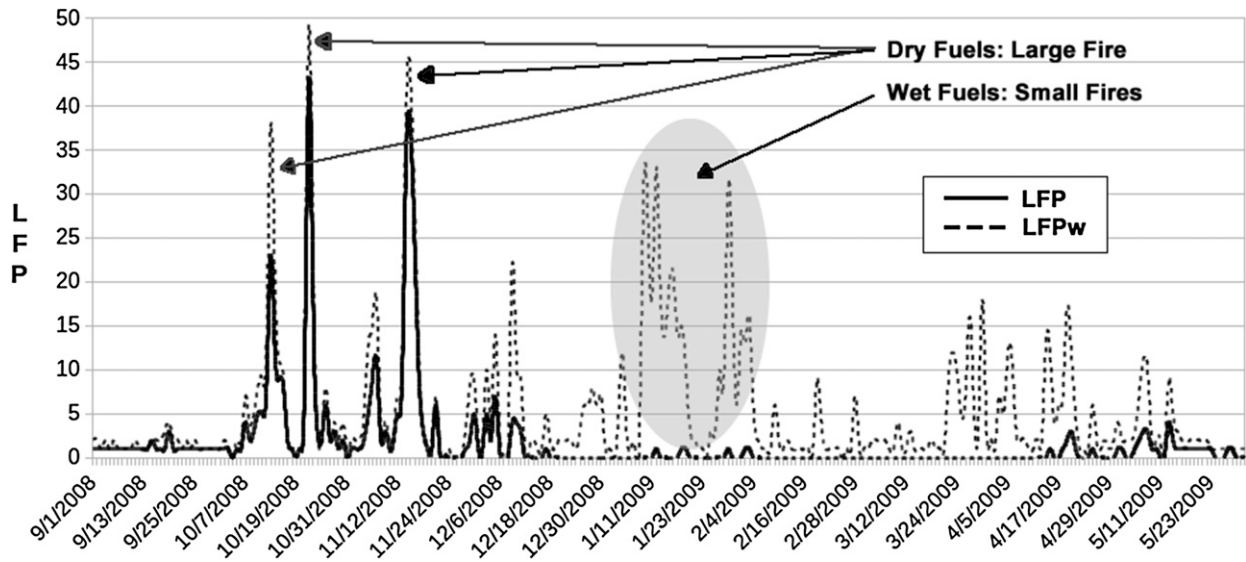


FIG. 6. Comparison of LFP_w and LFP time series for zone 1 during the period spanning September 2008–May 2009. For large fires that occurred in October and November of 2008, relatively dry fuels (LFP , solid black line) accompanied the dry and windy weather (LFP_w , dashed gray line). In contrast, January–February of 2009 experienced peaks of windy and dry conditions (LFP_w) accompanied by moist fuels (LFP) and, as a result, no fires grew larger than 100 ha.

at different temporal and horizontal resolutions ranging from hourly to daily, and from 3 to 12.5 km, respectively (Fig. 9). To reduce the exposure to error in fields with long accumulation periods, we sourced input variables for LFM and NDVI from the NLDAS-2 data (constructed using a land surface model in conjunction with assimilated observations and atmospheric model output). In contrast, hourly DFM and ERC values are predicted using offline models (Nelson 2000; Carlson et al. 2007; NFDRS) forced by WRF weather output.

DFM and ERC are calculated from meteorological variables predicted using WRF version 3.5 (Skamarock et al. 2008), run at 3- and 6-km horizontal resolution. We selected a WRF configuration that minimized errors

with respect to near-surface temperature, winds, and dewpoint during Santa Ana wind events (Cao 2015; Cao and Fovell 2016). This configuration includes the simple WRF single-moment 3-class microphysics scheme (Hong et al. 2004), the GCM version of the Rapid Radiative Transfer Model (RRTMG) shortwave and longwave radiation schemes (Iacono et al. 2008), the MM5 Monin–Obukhov surface layer scheme, and the Asymmetrical Convective Model version 2 boundary layer scheme (Pleim 2007). The Noah land surface model (Tewari et al. 2004) with four soil layers was used in conjunction with the MODIS land-use dataset. Each operational WRF forecast dynamically downscales the 12-km-resolution 0000 and 1200 UTC North American

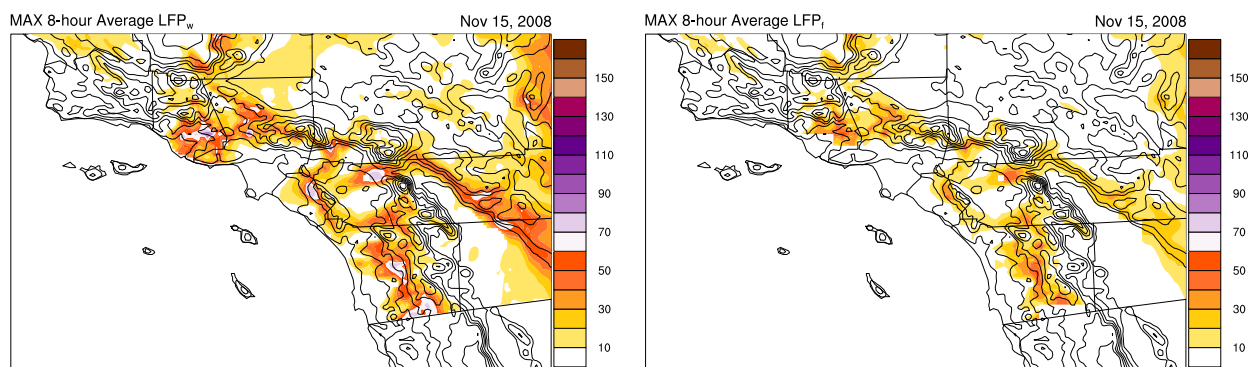


FIG. 7. Average (left) LFP_w and (right) LFP from 0800 to 1500 LST during a Santa Ana event on 15 Nov 2008. This offshore event was accompanied by the Freeway Complex fire, which burned over 12 141 ha, destroying 187 homes and damaging 117 others (http://cdfdata.fire.ca.gov/incidents/incidents_details_info?incident_id=305).

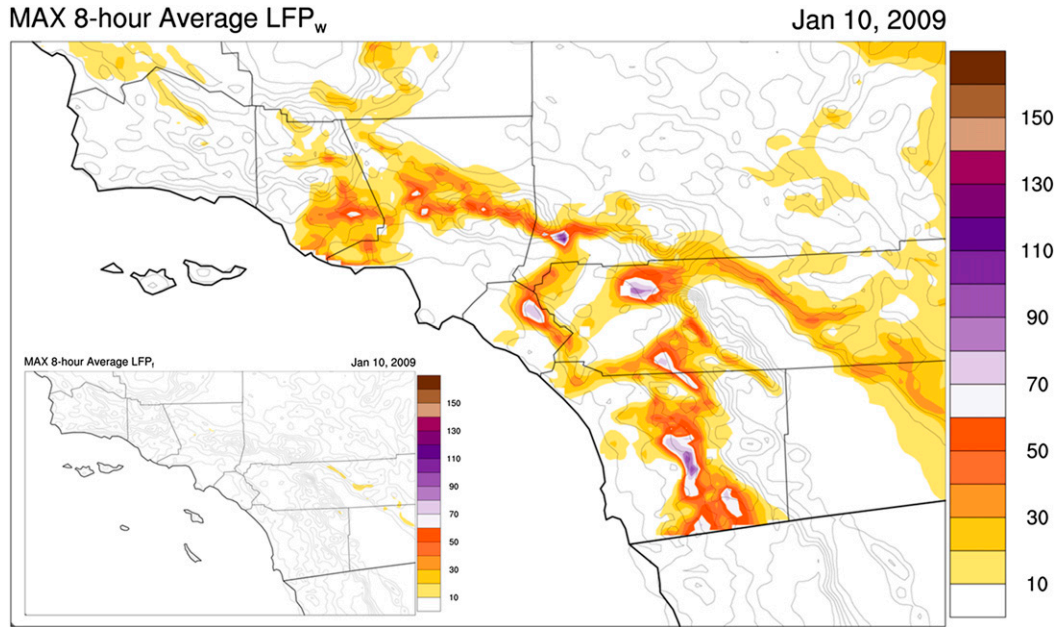


FIG. 8. Average LFP_w and (bottom left) LFP from 0800 to 1500 LST during a Santa Ana event in January 2009.

Mesoscale Forecast System (NAM) 1–3.5-day forecasts to 3-km resolution. We use a two-way-nested WRF domain configuration consisting of a 3-km-resolution innermost domain nested within a 9-km-resolution outermost domain with 51 vertical levels. To extend the forecast out to 6 days, the 0.25°-resolution Global Forecast System (GFS) is downscaled using WRF to 6-km resolution. We use a two-way-nested WRF domain

configuration consisting of a 6-km-resolution innermost domain nested within an 18-km outer domain and a 54-km outermost domain with 46 vertical levels. To help determine bounds and behavior of the SAWTI equations and place forecasts into some historical perspective, we dynamically downscaled the 32-km-resolution North American Regional Reanalysis (NARR; Mesinger et al. 2006) dataset to 3-km resolution using WRF over the

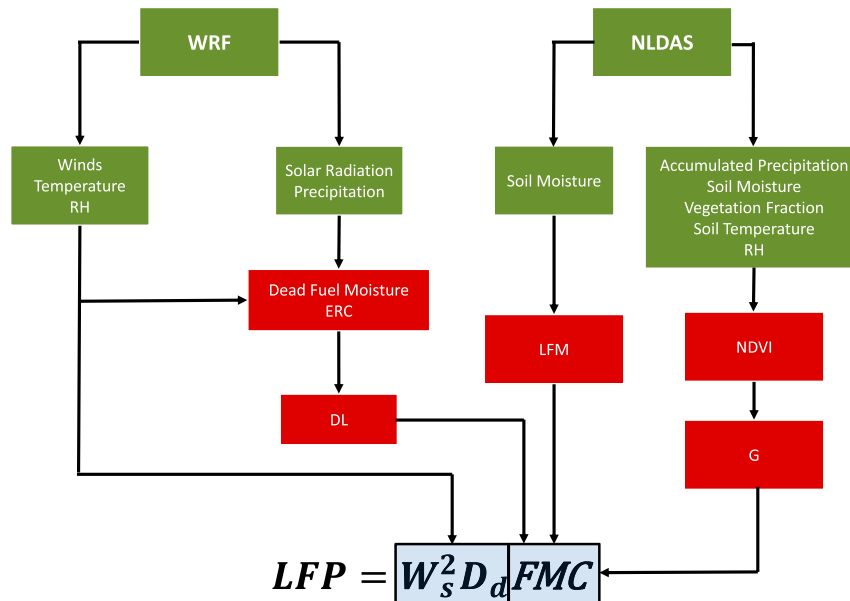


FIG. 9. Flowchart depicting operational LFP input models and datasets, derived variables, and the final LFP equation.

12 AM	1 AM	2 AM	3 AM	4 AM	5 AM	6 AM	7 AM	8 AM	9 AM	10 AM	11 AM	12 PM	1 PM	2 PM	3 PM	4 PM	5 PM	6 PM	7 PM	8 PM	9 PM	10 PM	11 PM
1								2								3							
4												5											

FIG. 10. Time periods over which LFP_w is averaged.

historical period spanning January 1984–December 2013. We used a two-way-nested WRF domain configuration consisting of a 27-km-resolution outer domain, 9-km-resolution inner domain, and 3-km-resolution innermost domain with 51 vertical levels. WRF was integrated across 3.5-day periods with the first 12 h from each period discarded as spinup time.

b. Calculating SAWTI

1) WEATHER

Equation (1) is temporally averaged at each WRF grid point across the domain using the following equation:

$$LFP_{w,gpx} = \frac{LFP_{w,hour1} + LFP_{w,hour2} + \dots + LFP_{w,hour8}}{8}, \quad (7)$$

where LFP_{w,gpx} is an average LFP_w value over an 8-h time period at grid point *x*. An 8-h period was chosen because that is ample time for the finer fuels (i.e., DFM_{10hr}) to respond to the ambient atmospheric conditions. Once

an average LFP_w had been calculated for each grid point, the maximum 8-h-average LFP_w for each day is then spatially averaged over each zone as follows:

$$LFP_{w,zone} = \frac{LFP_{wgp1} + LFP_{wgp2} + \dots + LFP_{wgpX}}{\text{Number of grid points per zone}}, \quad (8)$$

where LFP_{w,zone} is the maximum 8-h average at each grid point within the model domain. It is important to note that (7) was calculated for five different eight-consecutive-hour time periods with the highest value chosen to represent each zone for the day (Fig. 10). This is to ensure that the worst conditions are being captured on a daily basis. For instance while most Santa Ana wind events peak during the morning hours, some events can peak later in the day or at night depending on the arrival time of stronger dynamical support. Thus, calculating LFP_w for only one consecutive 8-h time period may fail to capture the worst conditions of the day. This more simplistic approach was favored compared to using an 8-h running average.

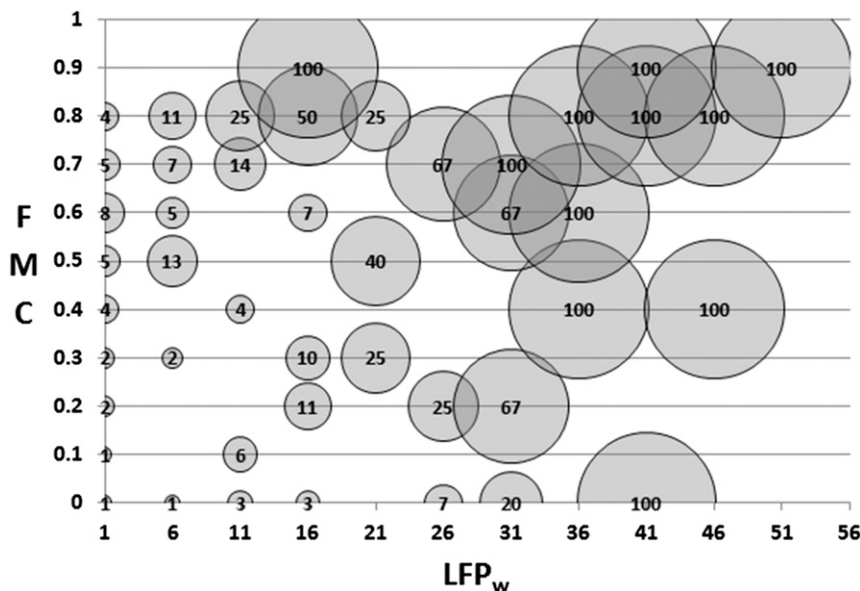


FIG. 11. Using historical fire occurrence data between 1992 and 2011, the relationship between binned FMC, LFP_w, and fire activity for zone 1 is shown. Tick marks indicate starting bin values for both FMC (bin interval of 0.099) and LFP_w (bin interval of 5). Bubble size indicates the conditional probability for an ignition to meet or exceed 100 ha. For instance, 100% of fires that ignited during conditions characterized by FMC ≥ 0.7 and LFP_w ≥ 36 grew into large fires.

TABLE 3. Categories of threat levels and their descriptions.

Category	Description
No rating	Santa Ana winds are either not expected or will not contribute to significant fire activity
Marginal	Upon ignition, fires may grow rapidly
Moderate	Upon ignition, fires will grow rapidly and will be difficult to control
High	Upon ignition, fires will grow very rapidly, will burn intensely, and will be very difficult to control
Extreme	Upon ignition, fires will have extreme growth, will burn very intensely, and will be uncontrollable

2) FUELS

Recall that DL relates ERC and DFM to historical fire activity. To provide a DL forecast, DFM and ERC are computed across the spunup WRF forecast period. To avoid the potentially long spinup times required by DFM, the DFM must be initialized at each grid point across the WRF domain. Since a publicly available gridded observed DFM product does not exist, DFM is initialized using the previous day’s DFM forecast valid at the fourth hour of the current WRF forecast. The first 4h of each WRF forecast are removed to allow for model spinup and to avoid contamination of DFM and

ERC as a result of relatively unrealistic atmospheric inputs. Because of the need for these continuously spunup DFM time series, WRF forecasts must be uninterrupted. However, if any WRF forecasts are missed, DFM forecasts could be initialized using output from earlier WRF/DFM forecasts, which are archived for at least a month.

Quasi-observational data (NLDAS-2) are available for estimating LFM and NDVI using (3) and (5), respectively. The 22-day lagged soil moisture required for LFM is provided from the Noah land surface model output of the NLDAS-2 dataset. For NDVI, the latest NLDAS-2 output is used (typically a 5-day lag),

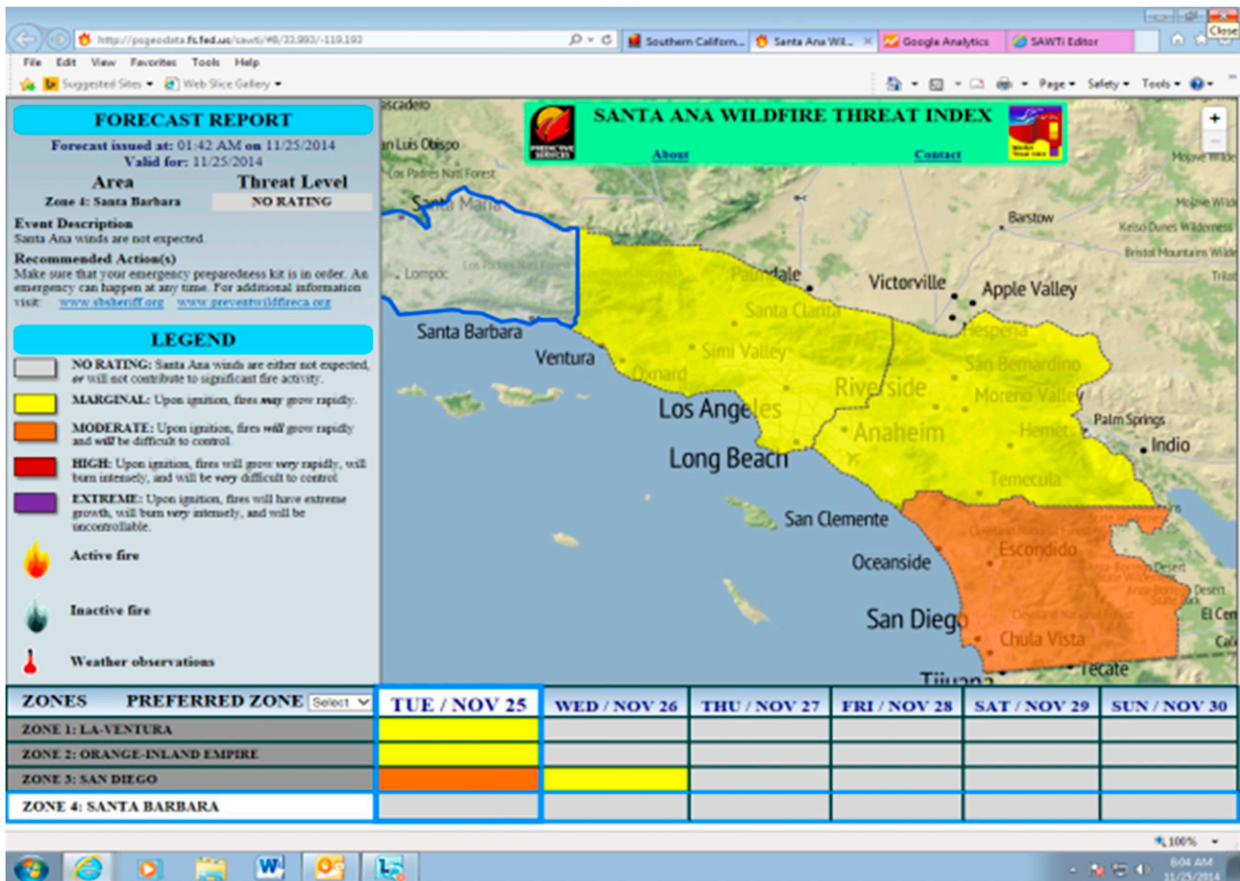


FIG. 12. Online operational SAWTI product.

which provides vegetation fraction, 2-m relative humidity, and soil moisture. Archived NLDAS-2 data are needed going back to the previous 1 September for cumulative precipitation. Both LFM and NDVI are regridded from the NLDAS-2 data at 12.5 km to the 3-km horizontal resolution, matching the WRF domain using bilinear interpolation, and are held constant across the 6-day forecast period. In contrast to weather that is calculated hourly, fuel conditions are calculated only at 1300 LST, representing fuel conditions for the entire day.

c. Public dissemination

Social science was incorporated during the early stages of the developmental process of SAWTI (Wall et al. 2014). The Desert Research Institute provided a social scientist to conduct an in-depth survey of five communities across Southern California. Much of the survey centered on questions regarding how the public obtains weather and fire information and their associated responses to that information. The results of the survey were used to help determine the type of information that would be presented in the product. In conjunction with the social science, historical weather and fuels data were correlated to historical fire occurrence records to develop index threat level categories. For example, for each SAWTI zone we compared daily FMC values along with daily LFP_w values from (1) for the historical period (1992–2011) to whether or not a fire had occurred. We repeated the process; this time equating the output to whether or not a 100-ha fire or greater occurred (Fig. 11). Comparing these two results yielded a conditional probability for an ignition to reach or exceed 100 ha based on FMC and LFP values. By assessing and employing these probabilities, LFP breakpoints could easily be determined (see section 3e for more details).

The SAWTI has four threat levels that range from “marginal” to “extreme.” When Santa Ana winds are either not expected or will not contribute to significant fire activity, then a “no rating” is issued for that day. For example, it could be possible that if a strong Santa Ana wind event were to transpire after appreciable rains occurred or when fuels are wet, the event would be categorized as a no rating. For definitions of other threat levels, see Table 3. Tied to each threat level is a list of recommended actions suggested to the public to better prepare for an impending event. Examples include the following instructions: “Clean debris away from your house, charge your cell phone and make sure you have plenty of gas.” The list of recommended actions expands as the threat levels increase. This aspect of the product is critical, as it serves to link categories of severity with public awareness.

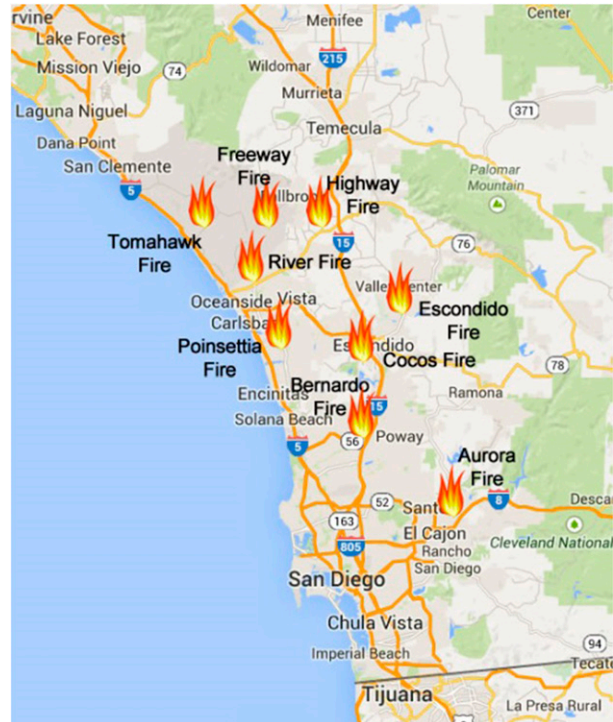


FIG. 13. Map of active fires (icons) on 14 May 2014 across San Diego County.

The product consists of an online web page (<http://sawti.fs.fed.us>) that displays a 6-day forecast of the above-mentioned categories for each of the four zones across Southern California (Fig. 12). A map of the region stands as the centerpiece of the page and graphically shows the categories that are colorized, ranging from gray (no rating) to purple (extreme). The product is issued once daily but can be updated more frequently as conditions warrant. The web page allows users to obtain more information such as viewing the latest weather observation from select stations when zoomed in on the map. The page will also display active and nonactive fires (via icons) on the map when such activity is present. Selecting one of these icons will provide the user with specific fire information such as acreage burned, percent contained, and links to more data. SAWTI also has a Twitter feed (https://twitter.com/sawti_forecast), where users are notified about changes in threat levels.

The product was beta tested for a year prior to it becoming a public product in the fall of 2014. During the beta test phase, the index performed well in capturing all events that occurred during the fall of 2013 through the spring of 2014, which featured events that ranged from no rating to high. Several notable events occurred during this period: 16 January 2014 (Colby fire), 29 April–1 May 2014 (Etiwanda fire), and 13–14 May 2014 (the

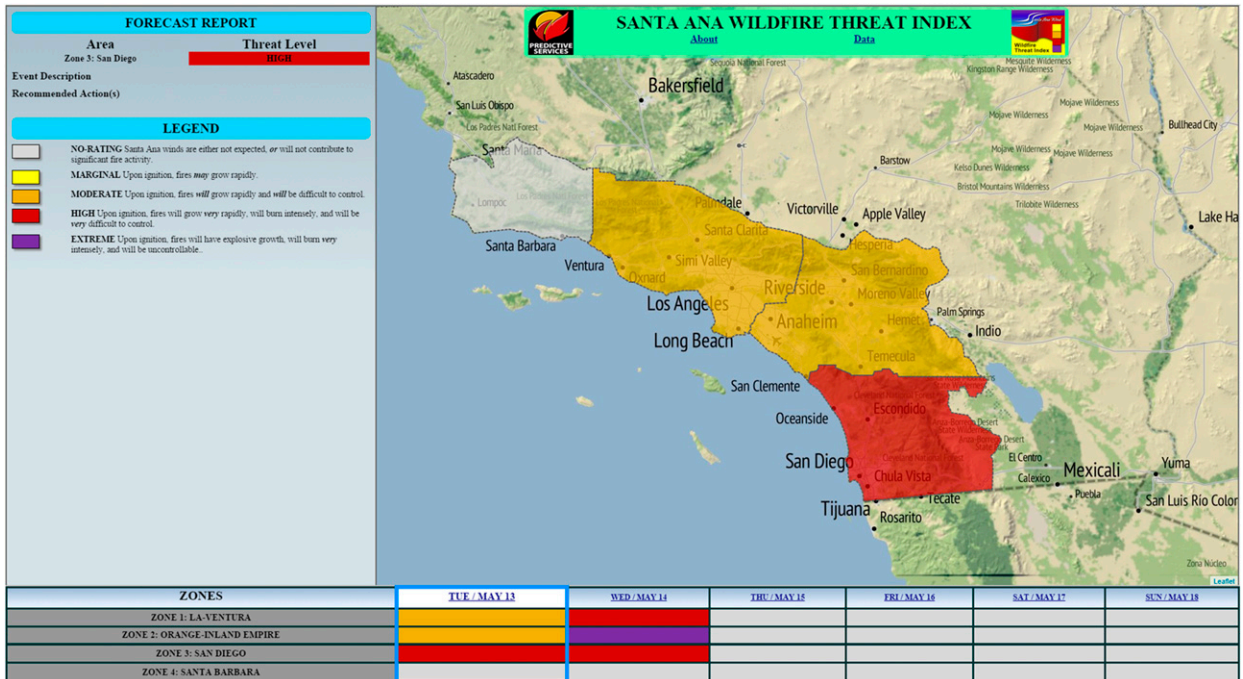


FIG. 14. SAWTI (in beta test) during 14–15 May 2014.

San Diego fires). Fire agencies that were granted access to the index during this time used the product to make critical decisions regarding the allocation and mobilization of shared fire resources prior to when these fires occurred. Specifically, the event that occurred on 13–14 May 2014 was especially notable because of the fact that the winds were unusually strong during this period, and that multiple large fires occurred as a result. Figure 13 shows a map of the fires across San Diego County, while Fig. 14 shows the SAWTI in beta test form for this event. The product was officially released to the public on 17 September 2014 via a press release and at an associated press conference. Since that time, the product has been used by local news media across the San Diego and Los Angeles metropolitan areas, as well as being shown on The Weather Channel.

d. Validation

Fire potential is very difficult to validate since our model is based on a conditional probability (i.e., getting an ignition). In addition, once an ignition occurs there are a number of human behaviors that cannot be predicted that can influence fire potential. For instance, if the SAWTI indicates a high likelihood of having a large fire for a particular Santa Ana wind event and one does not occur, it does not necessarily mean the model performed poorly. There may not have been an ignition during the event, or there may have been an ignition, but

adequate fire-fighting resources were made available to be successful in suppressing the incident before the fire became large. There have been a few times where the index displayed a no rating and a large fire occurred, but this has been very rare.

Modeling fuel conditions accurately presents certain challenges. Regarding DFM, our ability to validate WRF DFM and ERC is limited given the sparse observations across this domain. Various Remote Automated Weather Stations (RAWSSs) calculate DFM using measured atmospheric inputs including near-surface temperature, relative humidity, precipitation, and solar radiation. We validate WRF DFM and ERC across two years of the 30-yr historical period at 14 RAWSSs (Fig. 15). These stations were selected so that at least three stations represent zones 1–3. Zone 4 has relatively fewer RAWSSs reporting DFM and ERC measurements for the time period of interest; thus, only one station represents zone 4. At each RAWSS location, the closest WRF grid cell with the smallest elevation difference was selected for validation. We show two example time series plots (Figs. 16 and 17), for the Goose Valley and Claremont RAWSSs. At the Goose Valley RAWSS site (Fig. 16), the WRF DFM and ERC output agrees well with RAWSS measurements for most of the two years examined, with only slightly positive biases of 0.24 and 2.14 for DFM_{100hr} and DFM_{1000hr}, respectively. At the Claremont RAWSS (Fig. 17), the WRF DFM and ERC

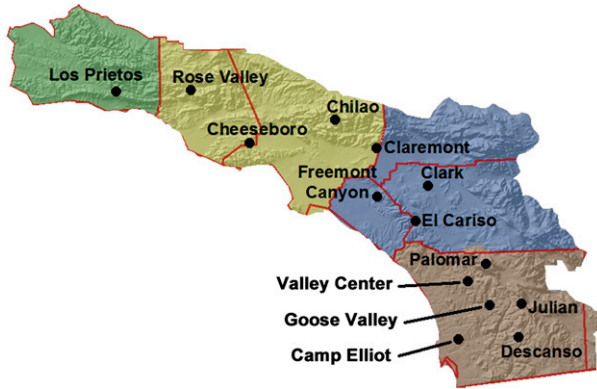


FIG. 15. RAWs used to validate WRF DFM and ERC.

output compares less favorably at certain times over the two years and more strongly during others. However, we report small biases at the Claremont RAWs of -1.27 and 1.30 for DFM_{100hr} and DFM_{1000hr} , respectively, with RMSEs of 4.22 and 2.65 . Table 4 shows WRF error statistics for all 14 RAWs across the 2-yr period. The WRF DFM_{100hr} bias ranges from -1.27 to 4.00 , while RMSE ranges from 2.72 to 4.93 , with the correlation

ranging from 0.55 to 0.86 . Our WRF DFM_{1000hr} has a positive bias ranging from 1.30 to 6.00 , with RMSE spanning 2.50 – 6.15 , and the correlation from 0.54 to 0.92 . Finally, the WRF ERC bias is mostly negative given the positive DFM_{1000hr} bias ranging from -25.09 to 0.50 , with RMSE ranging from 9.52 to 27.41 , and the correlation from 0.53 to 0.90 . It is hypothesized that WRF does not adequately resolve the complex topography at the two RAWs that have the worst error statistics: Chilao and Palomar.

e. Climatology

The historical dataset described previously provides us with an unprecedented 30-yr climatology of the fuel and weather variables related to wildfires across the four SAWTI zones in Southern California. Having this dataset has allowed us first to create breakpoints within the raw SAWTI output necessary for the development of the four threat levels that are integral to the final public product. To do this, we correlated historical fire occurrence data with historical LFP values from the dataset to develop breakpoints for the SAWTI. Most of the breakpoints fell naturally, but with some minor

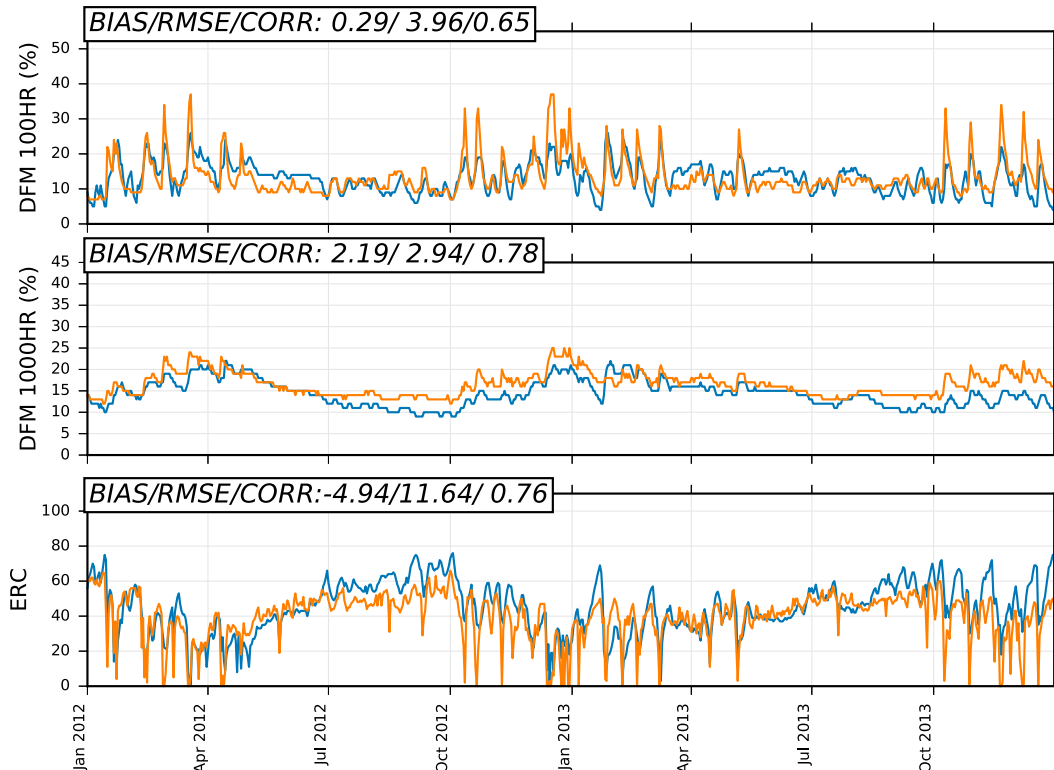


FIG. 16. RAWs (blue line) and closest WRF grid cell (orange line) time series of (top) 100- and (middle) 1000-h dead fuel moisture, and (bottom) ERC spanning January 2012–December 2013 for Goose Valley. WRF output coincides with RAWs 1300 LST measurements. Each plot is annotated with WRF output bias, RMSE, and the Spearman correlation.

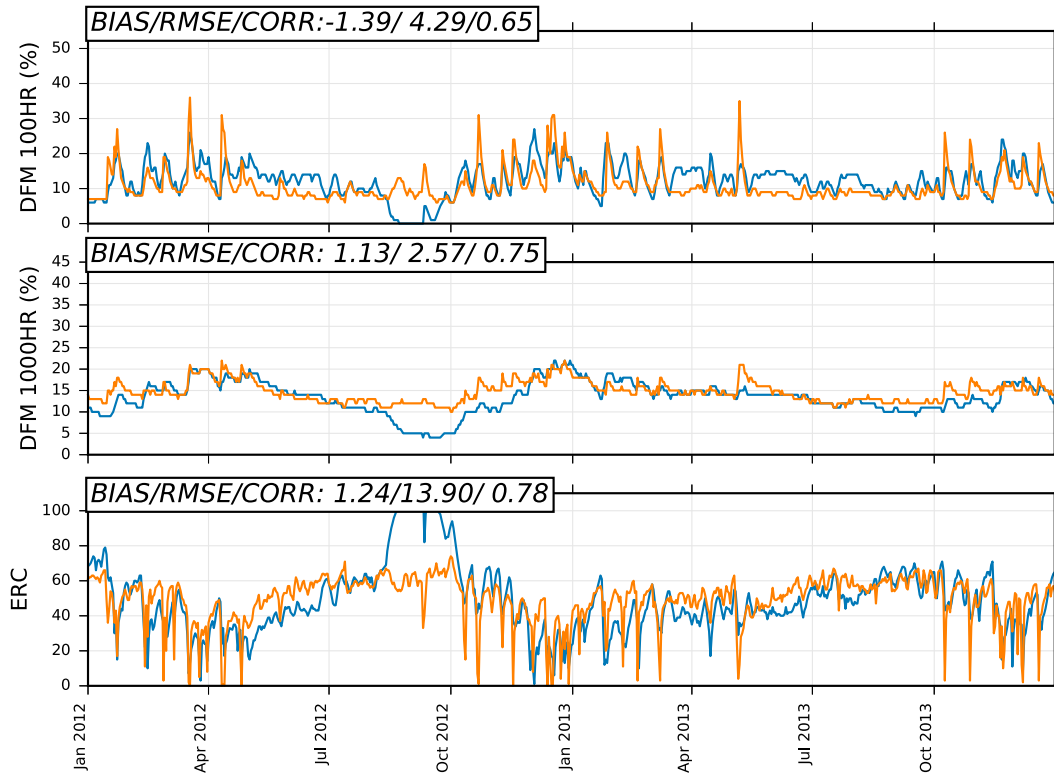


FIG. 17. As in Fig. 16, but for the Claremont RAWS.

adjustments, we created breakpoints at the 50th, 75th, 90th, and 97th percentiles. Significant increases in conditional probabilities for each category seemed to confirm our choices.

This unique dataset informs us about the historical significance the fuels, weather, and SAWTI events have had during the past 30 years. Having the ability to put past, but perhaps more importantly, forecasted SAWTI events into historical perspective helps inform the

public and first responders about the nature and the characteristics of an impending event. For example, we can authoritatively state that the Santa Ana wind event that helped to spawn the Witch Creek fire (and served as the catalyst for the development of this index) was ranked as the highest event in the 30-yr dataset for zones 1 and 2.

As we continue to explore this dataset, we hope to gain a better understanding of the climatology of Santa

TABLE 4. WRF error statistics at each RAWS for time spanning January 2012–December 2013.

Station	100-h DFM			1000-h DFM			ERC		
	Bias	RMSE	Correlation	Bias	RMSE	Correlation	Bias	RMSE	Correlation
Camp Elliot	0.17	3.90	0.55	1.75	2.97	0.54	-0.71	11.12	0.53
Cheeseboro	0.99	3.30	0.69	3.89	4.25	0.75	-10.78	14.81	0.74
Chilao	4.00	4.93	0.84	6.00	6.15	0.92	-25.09	27.41	0.89
Claremont	-1.27	4.22	0.66	1.30	2.65	0.76	0.50	13.71	0.79
Clark	-0.06	3.24	0.69	2.80	3.39	0.75	-4.27	11.24	0.76
Descanso	2.45	4.07	0.82	3.93	4.40	0.85	-14.40	18.39	0.84
El Cariso	1.26	3.70	0.73	3.27	3.94	0.81	-9.19	15.02	0.82
Fremont Canyon	-0.03	3.73	0.66	2.21	3.13	0.63	-2.52	11.25	0.73
Goose Valley	0.24	3.96	0.65	2.14	2.90	0.78	-4.82	11.50	0.77
Julian	0.95	3.97	0.80	2.36	3.05	0.90	-4.81	10.54	0.90
Los Prietos	-0.97	2.72	0.74	1.69	2.67	0.72	-3.27	10.45	0.72
Palomar	3.06	4.46	0.86	4.12	4.82	0.88	-14.72	20.12	0.88
Rose Valley	0.74	2.83	0.77	3.06	3.45	0.85	-10.06	14.06	0.82
Valley Center	-0.22	3.80	0.67	1.84	2.50	0.80	-2.32	9.52	0.78

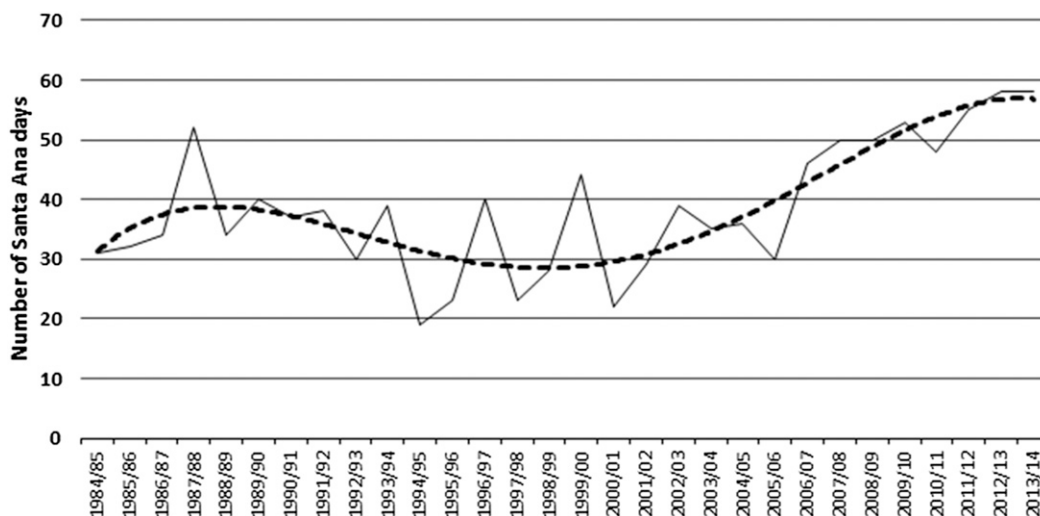


FIG. 18. Number of Santa Ana wind days per rain year (1 Jul–30 Jun) for years spanning 1984–2014 (solid black line). Dashed line is a polynomial fit to the data, which helps to depict the longer time period trends.

Ana winds during the past three decades, including detecting and understanding interannual trends and cycles in event frequencies and strength. Figure 18 shows the number of days when Santa Ana winds occurred across zone 3 for the period spanning 1984–2013. This figure reveals a noticeable upward trend in the frequency of Santa Ana wind days during approximately the last 10 years, ending in 2013. Preliminary research shows that this long-term trend in frequency (possibly associated with a longer-term interannual cycle) coincides with a predominately negative phase of the Pacific decadal oscillation (PDO). Further investigation conducted in a future paper will seek to explore the causal mechanisms for this trend in frequency, as well as other trends in Santa Ana wind characteristics.

4. Summary and conclusions

As the wildland–urban interface (WUI) continues to expand across Southern California, the sources of ignition will increase, leading to a greater probability for large and destructive fires during Santa Ana wind events. This puts the public and firefighter safety at risk, thus the increasing need to categorize such events in terms of their effect on the fire environment.

Predictive Services' initial efforts to categorize Santa Ana winds helped to provide the leadership and guidance necessary for the development of the SAWTI. Through the successful collaboration between the government, academia, and the private sector, high-resolution model data along with satellite-derived variables allowed us to incorporate fuel and weather data into the index on a gridded domain within Southern California. Challenges

surrounding the assessment of fuel conditions include the difficulty in determining different fuel moisture parameters, which can sometimes result in a less accurate evaluation of fuel conditions. Further refinement of the model is needed to improve the overall output. However, during the beta testing process, the index performed very well with positive responses from the recipients of the preliminary output. Since its public unveiling, the index has been well received by the media and the fire community.

Our 30-yr dataset is unprecedented. Not only does it provide us with 30 years' worth of fuel moisture data across Southern California (which is useful in relating fuel conditions with drought), it also gives us quantifiable outputs of average wind velocity, dewpoint depression, and the SAWTI itself. This allows us to put past and future Santa Ana events (magnitude, duration, and spatial coverage) into historical perspective, which is significant. Future studies in the climatology of such events can be conducted, leading to a better understanding of why certain trends exist.

Fire agencies and first responders, private industry, the general public, and the media now have a new operational tool that determines the severity of Santa Ana wind events. Furthermore, they will have a clearer understanding of the severity of an event based on the potential for large fires to occur. Specifically, a more effective media response will result in the general population (particularly those living within the WUI) being more proactive in its response to an impending event.

Acknowledgments. The authors thank Dr. Jim Means for his helpful suggestions and input into this project.

We also appreciate the advice from Beth Hall, Tamara Wall, Mark Jackson, and Alex Tardy. The data used in this study were acquired as part of the mission of NASA's Earth Science Division and archived and distributed by the Goddard Earth Sciences (GES) Data and Information Services Center (DISC). Major funding for this project was provided by SDG&E.

REFERENCES

- Blier, W., 1998: The sundowner winds of Santa Barbara, California. *Wea. Forecasting*, **13**, 702–716, doi:10.1175/1520-0434(1998)013<0702:TSWOSB>2.0.CO;2.
- Bradshaw, L. S., R. E. Burgan, J. D. Cohen, and J. E. Deeming, 1983: The 1978 National Fire Danger Rating System: Technical documentation. General Tech. Rep. INT-169, Intermountain Forest and Range Experiment Station, U.S. Forest Service, 44 pp. [Available online at http://www.fs.fed.us/rm/pubs_int/int_gtr169.pdf.]
- Cao, Y., 2015: The Santa Ana winds of Southern California in the context of fire weather. Ph.D. thesis, University of California, Los Angeles, 172 pp.
- , and R. G. Fovell, 2016: Downslope windstorms of San Diego County. Part I: A case study. *Mon. Wea. Rev.*, **144**, 529–552, doi:10.1175/MWR-D-15-0147.1.
- Carlson, J. D., L. S. Bradshaw, R. M. Nelson Jr., R. R. Bensch, and R. Jabrzemski, 2007: Application of the Nelson model to four timelag fuel classes using Oklahoma field observations: Model evaluation and comparison with National Fire Danger Rating System algorithms. *Int. J. Wildland Fire*, **16**, 204–216, doi:10.1071/WF06073.
- Castro, F. X., A. Tudela, and M. Sebasti a, 2003: Modeling moisture content in shrubs to predict fire risk in Catalonia (Spain). *Agric. For. Meteorol.*, **116**, 49–59, doi:10.1016/S0168-1923(02)00248-4.
- Chuvieco, E., D. Cocero, D. Ria o, P. Martin, J. Mart inez-Vega, J. de la Riva, and F. P erez, 2004: Combining NDVI and surface temperature for the estimation of live fuel moisture content in forest fire danger rating. *Remote Sens. Environ.*, **92**, 322–331, doi:10.1016/j.rse.2004.01.019.
- Clinton, N. E., C. Potter, B. Crabtree, V. Genovese, P. Gross, and P. Gong, 2010: Remote sensing-based time-series analysis of cheatgrass (*bromus tectorum* L.) phenology. *J. Environ. Qual.*, **39**, 955–963, doi:10.2134/jeq2009.0158.
- Countryman, C. M., and C. W. Philpot, 1970: Physical characteristics of chamise as a wildland fuel. USDA Forest Service Research Paper PSW-66, 16 pp. [Available online at http://www.fs.fed.us/psw/publications/documents/psw_rp066/psw_rp066.pdf.]
- Elmore, A. J., J. F. Mustard, S. J. Manning, and D. B. Lobell, 2000: Quantifying vegetation change in semiarid environments: Precision and accuracy of spectral mixture analysis and the normalized difference vegetation index. *Remote Sens. Environ.*, **73**, 87–102, doi:10.1016/S0034-4257(00)00100-0.
- Fosberg, M. A., 1978: Weather in wildland fire management: the fire weather index. *Proc. Conf. on Sierra Nevada Meteorology*, Lake Tahoe, CA, Amer. Meteor. Soc., 1–4.
- Hong, S.-Y., J. Dudhia, and S.-H. Chen, 2004: A revised approach to ice microphysical processes for the bulk parameterization of clouds and precipitation. *Mon. Wea. Rev.*, **132**, 103–120, doi:10.1175/1520-0493(2004)132<0103:ARATIM>2.0.CO;2.
- Hughes, M., and A. Hall, 2010: Local and synoptic mechanisms causing Southern California's Santa Ana winds. *Climate Dyn.*, **34**, 847–857, doi:10.1007/s00382-009-0650-4.
- Iacono, M. J., J. S. Delamere, E. J. Mlawer, M. W. Shephard, S. A. Clough, and W. D. Collins, 2008: Radiative forcing by long-lived greenhouse gases: Calculations with the AER radiative transfer models. *J. Geophys. Res.*, **113**, D13103, doi:10.1029/2008JD009944.
- Jin, Y., and Coauthors, 2015: Identification of two distinct fire regimes in Southern California: Implications for economic impact and future change. *Environ. Res. Lett.*, **10**, 094005, doi:10.1088/1748-9326/10/9/094005.
- Mesinger, F., and Coauthors, 2006: North American Regional Reanalysis. *Bull. Amer. Meteor. Soc.*, **87**, 343–360, doi:10.1175/BAMS-87-3-343.
- Moritz, M. A., T. J. Moody, M. A. Krawchuck, M. Hughes, and A. Hall, 2010: Spatial variation in extreme winds predicts large wildfire location in chaparral ecosystems. *Geophys. Res. Lett.*, **37**, L04801, doi:10.1029/2009GL041735.
- Nelson, R. M., Jr., 2000: Prediction of diurnal change in 10-h fuel stick moisture content. *Can. J. For. Res.*, **30**, 1071–1087, doi:10.1139/x00-032.
- Pleim, J. E., 2007: A combined local and nonlocal closure model for the atmospheric boundary layer. Part I: Model description and testing. *J. Appl. Meteor.*, **46**, 1383–1395, doi:10.1175/JAM2539.1.
- Pollet, J., and A. Brown, 2007: Fuel moisture sampling guide. Utah State Office, Bureau of Land Management, Salt Lake City, UT, 32 pp. [Available online at <http://www.wfas.net/nfmd/references/fmg.pdf>.]
- Preisler, H. K., S. C. Chen, F. Fujioka, J. W. Benoit, and A. L. Westerling, 2008: Wildland fire probabilities estimated from weather model-deduced monthly mean fire danger indices. *Int. J. Wildland Fire*, **17**, 305–316, doi:10.1071/WF06162.
- Raphael, M. N., 2003: The Santa Ana winds of California. *Earth Interact.*, **7**, doi:10.1175/1087-3562(2003)007<0001:TSAWOC>2.0.CO;2.
- Rolinski, T., D. Eichhorn, B. J. D'Agostino, S. Vanderburg, and J. D. Means, 2011: Santa Ana forecasting and classification. *2011 Fall Meeting*, San Francisco, CA, Amer. Geophys. Union, Abstract NH33B-1573.
- Rothermel, R. C., 1972: A mathematical model for predicting fire spread in wildland fuels. USDA Forest Service Research Paper INT-115, 40 pp. [Available online at http://www.fs.fed.us/rm/pubs_int/int_rp115.pdf.]
- Skamarock, W. C., and Coauthors, 2008: A description of the Advanced Research WRF version 3. NCAR Tech. Note NCAR/TN-475+STR, 113 pp., doi:10.5065/D68S4MVH.
- Tewari, M., and Coauthors, 2004: Implementation and verification of the unified Noah land surface model in the WRF model. Preprints, *Conf. on Weather Analysis and Forecasting/16th Conf. on Numerical Weather Prediction*, Seattle, WA, Amer. Meteor. Soc., 14.2a. [Available online at https://ams.confex.com/ams/84Annual/techprogram/paper_69061.htm.]
- Wall, T. U., A. L. Knox Velez, and J. Diaz, 2014: Wildfire readiness in the Southern California wildland-urban interface. Desert Research Institute Research Rep., 16 pp. [Available online at <http://www.dri.edu/dripublications>.]
- White, M. A., P. E. Thornton, and S. W. Running, 1997: A continental phenology model for monitoring vegetation responses to inter-annual climatic variability. *Global Biogeochem. Cycles*, **11**, 217–234, doi:10.1029/97GB00330.